$$\varepsilon_x = \frac{\sigma_x}{E_x} - \frac{\nu_{xy}\sigma_y}{E_y} - \frac{\nu_{yz}\sigma_z}{E_z} \quad (4)$$

$$\varepsilon_y = -\frac{\nu_{xy}\sigma_x}{E_y} + \frac{\sigma_y}{E_y} - \frac{\nu_{yz}\sigma_z}{E_z} \quad (5)$$

$$\varepsilon_z = -\frac{\nu_{yz}\sigma_x}{E_z} - \frac{\nu_{yz}\sigma_y}{E_z} + \frac{\sigma_z}{E_z} \quad (6)$$

To determine E_y and E_z, ν_{xy} and ν_{yz}, four equations are required. Two loading cases as shown in figure 22 have been designed to give four such equations based on the theory of elasticity. For load case (figure 2a), the stress and strain components on the lateral surface are:

$\sigma_x = \sigma_y = 0$

$\varepsilon_x = \frac{\Delta a}{a}$ along $x = \pm a$ and $\varepsilon_y = \frac{\Delta a}{a}$ along $y = \pm a$

$\varepsilon_z = \frac{\Delta a}{a}$

where Δa is the change of dimension a of cross-section under the stretch Δa in the z-direction. Integrating and averaging Eq. (6) on the plane z = a, the following equation can be arrived:

$$E_z = \frac{\sigma_{ave}}{\varepsilon_z} = \frac{a}{\Delta a}\sigma_{ave} \quad (7)$$

where the average value of σ_z is given by:

$$\sigma_{ave} = \iint \sigma_z(x, y, a)\,dxdy \quad (8)$$

The value of σ_{ave} is evaluated for the RVE using finite element analysis (FEA) results.

Using Eq. (5) and the result (7), the strain along $y = \pm a$:

$$\varepsilon_y = -\frac{\nu_{yz}\sigma_z}{E_z} = -\nu_{yz}\frac{\Delta a}{a} = \frac{\Delta a}{a}$$

Hence, the expression for the Poisson's ratio ν_{yz} is as follows:

$$\nu_{yz} = -1 \quad (9)$$

For load case (figure 2b), the square representative volume element (RVE) is loaded with a uniformly distributed load (negative pressure), P in a lateral direction, for instance, the x-direction. The RVE is constrained in the z-direction so that the plane strain condition is sustained to simulate the interactions of RVE with surrounding materials in the z-direction. Since, $\varepsilon_z = 0$, $\sigma_z = \nu_{yz}(\sigma_x + \sigma_y)$ for the plain stress, the strain-stress relations can be reduced as follows:

$$\varepsilon_x = \left(\frac{1}{E_x} - \frac{1}{E_z}\right)\sigma_x - \left(\frac{\nu_{xy}}{E_y} + \frac{1}{E_z}\right)\sigma_y \quad (10)$$

$$\varepsilon_y = -\left(\frac{\nu_{xy}}{E_x} + \frac{1}{E_z}\right)\sigma_x + \left(\frac{1}{E_x} - \frac{1}{E_z}\right)\sigma_y \quad (11)$$

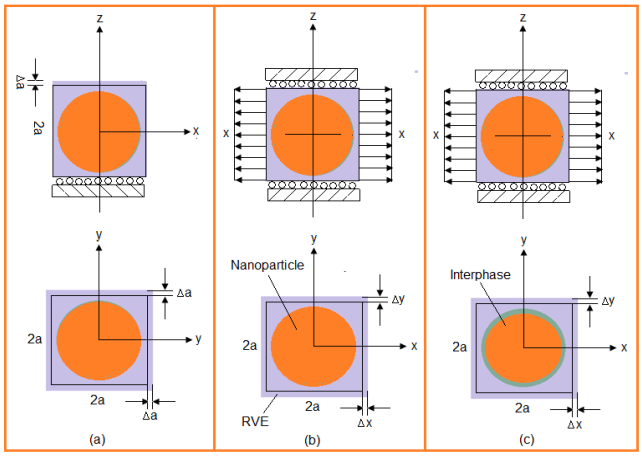

Figure 2: RVE models

For the elasticity model as shown in figure 2b, one can have the following results for the normal stress and strain components at a point on the lateral surface:

$\sigma_y = 0$, $\sigma_x = P$

$\varepsilon_x = \frac{\Delta x}{a}$ along $x = \pm a$ and $\varepsilon_y = \frac{\Delta y}{a}$ along $y = \pm a$

where Δx (>0) and Δy (<0) are the changes of dimensions in the x- and y- direction, respectively for the load case shown in Fig.2b. Applying Eq. (11) for points along $y = \pm a$ and Eq. (10) for points along $x = \pm a$, we get the following:

$$\varepsilon_y = -\left(\frac{\nu_{xy}}{E_x} + \frac{1}{E_z}\right)P = \frac{\Delta y}{a} \quad (12)$$

$$\varepsilon_x = \left(\frac{1}{E_x} - \frac{1}{E_z}\right)P = \frac{\Delta x}{a} \quad (13)$$

By solving Eqs. (12) and (13), the effective elastic modulus and Poisson's ratio in the transverse direction (xy-plane) as follows:

$$E_x = E_y = \frac{1}{\frac{\Delta x}{Pa} + \frac{1}{E_z}} \quad (14)$$

$$\nu_{xy} = \left(\frac{\Delta y}{Pa} + \frac{1}{E_z}\right)\Big/\left(\frac{\Delta x}{Pa} + \frac{1}{E_z}\right) \quad (15)$$

In which E_z can be determined from Eq. (7). Once the change in lengths along x- and y- direction (Δx and Δy) are determined for the square RVE from the FEA, E_y (= E_x) and ν_{xy} can be determined from Eqs. (14) and (15), correspondingly.

The young's modulus of the interphase is obtained by the following formula:

$$E_i(r) = (\alpha E_p - E_m)\left(\frac{r_i - r}{r_i - r_p}\right) + E_m \quad (16)$$

3. Materials Methods

The matrix material was AA7175 aluminum alloy. AA7175 contains Si (12.50%), Cr (≤0.10%), Cu (1.20%), Fe (≤1.00%), Mg (1.10%), Ni (1.00%) and Zn (≤0.25%) as its major alloying elements. The reinforcement material was aluminum nitride (AlN) nanoparticles of average size 100nm. The mechanical properties of materials used in the present work are given in table 1.

Table 1: Mechanical properties of AA7175 matrix and AlN nanoparticles

Property	AA7175	AlN
Density, g/cc	2.68	3.26
Elastic modulus, GPa	78.6	330
Ultimate tensile strength, MPa	379	270
Poisson's ratio	0.33	0.24

In this research, a cubical RVE was implemented to analyze the tensile behavior AA7175/AlN nanocomposites (Fig.2c). The determination of the RVE's dimensional conditions requires the establishment of a volumetric fraction of spherical nanoparticles in the composite. Hence, the weight fractions of the particles were converted to volume fractions. The volume fraction of a particle in the RVE ($V_{p,rve}$) is determined using Eq.(17):

$$v_{p,rve} = \frac{\text{Volume of nanoparticle}}{\text{Volume of RVE}} = \frac{16}{3} \times \left(\frac{r}{a}\right)^3 \quad (17)$$

where, r represents the particle radius and a indicates the diameter of the cylindrical RVE. The volume fraction of the particles in the composite (V_p) is obtained using equation

$$V_p = (w_p/\rho_p)/(w_p/\rho_p + w_m/\rho_m) \quad (18)$$

where ρ_m and ρ_p denote the matrix and particle densities, and w_m and w_p indicate the matrix and particle weight fractions, respectively.

The RVE dimension (a) was determined by equalizing Eqs. (17) and (18). Two RVE schemes namely: without interphase (adhesion) and with interphase were applied between the matrix and the filler. The loading on the RVE was defined as symmetric displacement, which provided equal displacements at both ends of the RVE. To obtain the nanocomposite modulus and yield strength, the force reaction was defined against displacement. The large strain PLANE183 element [12] was used in the matrix and the interphase regions in all the models. In order to model the adhesion between the interphase and the particle, a COMBIN14 spring-damper element was used. The stiffness of this element was taken as unity for perfect adhesion which could determine the interfacial strength for the interface region.

It is equally important to set the strain rates of the finite element models based on the experimental tensile tests' setups to converge an exact nonlinear solution. Hence, FEM models of different RVEs with various particle contents should have comparable error values. In this respect, the ratio of the tensile test speed/the gauge length of the specimens should be the same as the corresponding ratio in the RVE displacement model. Therefore, the rate of displacement in the RVEs was set to be 0.1 (1/min).

4. Results and Discussion

The AlN/AA7175 nanocomposites with or without interphase were modeled using finite element analysis (ANSYS) to analyze the tensile behavior and fracture.

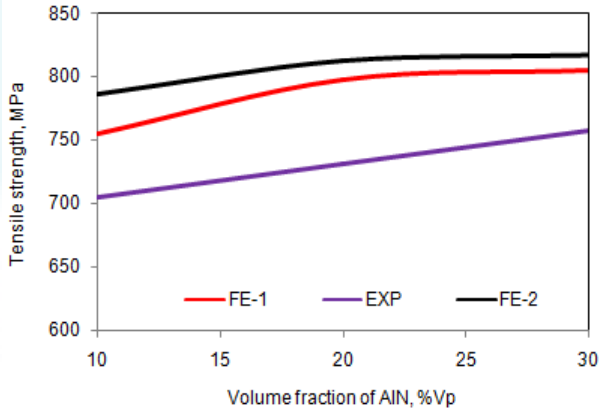

Figure 3: Effect of volume fraction on tensile strength along tensile load direction

4.1 Tensile behavior

An increase of AlN content in the matrix could increase the tensile strength of the nanocomposite (figure 3). The maximum difference between the FEA results without interphase and the experimental results was 66.89 MPa. This differentiation can be attributed to lack of bonding between the AlN nanoparticle and the AA7175 matrix. The maximum difference between the FEA results with interphase and the experiments results was 81.36 MPa. This discrepancy can be endorsed to the presence of voids in the nanocomposites.

For 10%, 20% and 30%Vp of AlN in AA7175, without interphase and barely consideration of adhesive bonding between the AlN nanoparticle and the AA7175 matrix, the loads transferred from the AlN nanoparticle to the AA7175 matrix were, respectively, 122.65 MPa, 192.58 MPa and 196.64 MPa (figure 4a) along the tensile load direction. Similarly, for 10%, 20% and 30%Vp of AlN in AA7175, with interphase and wetting between the ALN nanoparticle and the AA7175 matrix, the loads transferred from the AlN nanoparticle to the AA7175 matrix were, respectively,184.12 MPa, 252.66 MPa and 201.60 MPa (figure 4b) along the tensile load direction. Zhengang et al [13] carried a study improving wettability by adding Mg as the wetting agent. They suggested that the wettability between molten Al-Mg matrix and SiC particles is improved and the surface tension of molten Al-Mg alloy with SiC particle is reduced, and results in homogeneous particles distribution and high interfacial bond strength. For instance, addition of Mg to composite matrix lead to the formation of MgO and $MgAl_2O_3$ at the interface and this enhances the wettability and the strength of the composite [14].

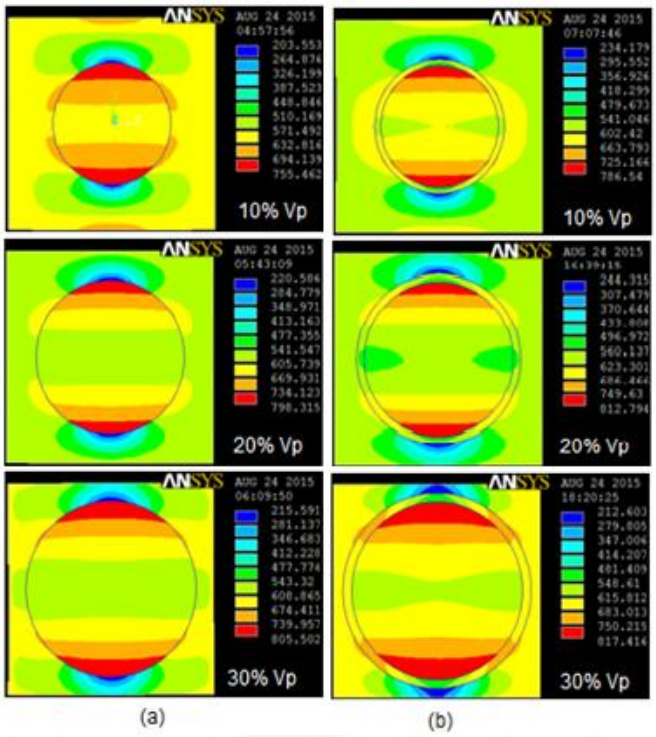

Figure 4: Tensile stresses (a) without interphase and (b) with interphase normal to load direction.

4.2 Fracture behavior

Figure 5 depicts the increase of von Mises stress with increase of volume fraction of AlN. In the case of nanocomposites with interphase between the nanoparticle and the matrix, the stress was transferred through shear from the matrix to the particles resulting low stress in the matrix. The stress transfer from the matrix to the nanoparticle was less for the nanocomposites without interphase resulting high stress in the matrix. Landis and McMeeking [15] assume that the fibers carry the entire axial load, and the matrix material only transmits shear between the fibers. Based on these assumptions alone, it is generally accepted that these methods will be most accurate when the fiber volume fraction V_f and the fiber-to matrix moduli ratio E_f /E_m are high. In the present case, the elastic moduli of AA7175 matrix and AlN nano particle are, respectively, 72.0 GPa and 330 GPa.

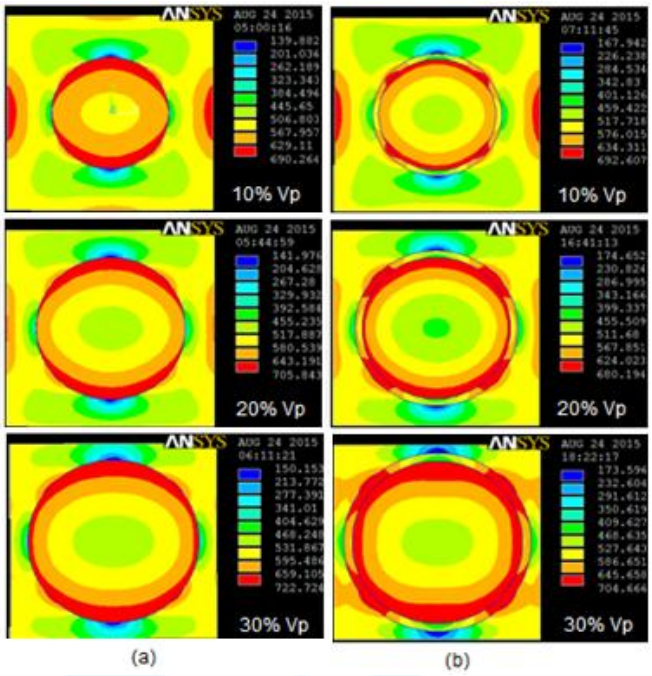

Figure 5: von Mises stress (a) and shear stress (b).

5. Conclusion

The RVE models give the trend of phenomenon happening in the nanocomposites. Without interphase and barely consideration of adhesive bonding, the tensile strength has been found to be 805.50 MPa for the nanocomposites consisting of 30%Aln nanoparticles. Due to interphase between the nanoparticle and the matrix, the tensile strength increases to 817.42 MPa. The tensile strengths obtained by author's model (with voids) are in good agreement with the experimental results. In the case of nanocomposites with interphase between the nanoparticle and the matrix, the stress is transferred through shear from the matrix to the particles. The transverse moduli of AlN/AA7175 nanocomposites have been found to be 20.64 GPa and 26.47 GPa, respectively, without and with interphase.

References

[1] A. C. Reddy, "Mechanical properties and fracture behavior of 6061/SiCp Metal Matrix Composites Fabricated by Low Pressure Die Casting Process," Journal of Manufacturing Technology Research, 1(3/4), 273-286, 2009.

[2] A. C. Reddy, Essa Zitoun, "Tensile properties and fracture behavior of 6061/Al_2O_3 metal matrix composites fabricated by low pressure die casting process," International Journal of Materials Sciences, 6(2), 147-157, 2011.

[3] X. Deng, N. Chawla, "Modeling the effect of particle clustering on the mechanical behavior of SiC particle reinforced Al matrix composites," Journal of Materials Science, 41, 5731–5734, 2006.

[4] A.J. Reeves, H. Dunlop, T.W. Clyne, "The effect of interfacial reaction layer thickness on fracture of titanium–SiC particulate composites," Metallurgical Transactions A, 23, 977–988, 1992.

[5] B. Kotiveerachari, A. C. Reddy, "Interfacial effect on the fracture mechanism in GFRP composites," In Proceedings of the CEMILAC Conference, Ministry of Defense, India, 1(B), pp.85-87, 1999.

[6] A. C. Reddy, "Analysis of the Relationship between the Interface Structure and the Strength of Carbon-Aluminum Composites," In the Proceedings of the NATCON-ME, Bangalore, pp.61-62, 2004.

[7] S. Ren, X. Shen, S. Qu, X. He, "Effect of Mg and Si on infiltration behavior of Al alloys pressureless infiltration into porous SiCp performs," International Journal Minerals, Metallurgy and Materials, 18 (6), 703–708, 2011.

[8] N. Sobczak, M. Ksiazek, W. Radziwill, J. Morgiel, W. Baliga, L. Stobierski, "Effect of titanium on wettability and interfaces in the Al/ SiC system," In Proceedings of the International Conference on High Temperature Capillarity, Cracow, Poland, 1997.

[9] A. M. Davidson, D. Regener, "A comparison of aluminum based metal matrix composites reinforced with coated and uncoated particulate silicon carbide," Composites Science and Technology, 60(6), 865-869, 2000.

[10] R. Hill, "Elastic properties of reinforced solids: some theoretical principles," Journal of the Mechanics and Physics of Solids, 11, 357-372, 1963.

[11] Y. J. Liu, X. L. Chen, "Evaluations of the effective material properties of carbon nanotube-based composites using a nanoscale representative volume element," Mechanics of Materials, 35, 69–81, 2003.

[12] Chennakesava R Alavala, Finite Element Methods: Basic Concepts and Applications, PHI Learning Pvt. Ltd, New Delhi, India, 2008.

[13] Z. Liuy, G. Zu, H. Luo, Y. Liu, G. Yao, "Influence of Mg Addition on Graphite Particle Distribution in the Al Matrix Composites," Journal of Materials Science & Technology, 26(3), 244, 244-250, 2010.

[14] A. C. Reddy, Essa Zitoun, "Matrix alloys for alumina particle reinforced metal matrix composites," Indian Foundry Journal, 55(1), 12-16, 2009.

[15] C. M. Landis, R. M. McMeeking, R.M, "Stress concentrations in composites with interface sliding, matrix stiffness, and uneven fiber spacing using shear lag theory," International Journal of Solids Structures, 41, 6289-6313, 1999.

Author Profile

Dr. A. Chennakesava Reddy, B.E., M.E (Prod). M.Tech (CAD/CAM)., Ph.D (prod)., Ph.D (CAD/CAM) is a Professor in Mechanical Engineering, Jawaharlal Nehru Technological University, Hyderabad. The author has published 279 technical papers worldwide. He is the recipient of best paper awards ten times. He is recipient of Best Teacher Award from the Telangana State, India. He has successfully completed several R&D and consultancy projects. He has guided 14 Research Scholars for their Ph.D. He is a Governing Body Member for several Engineering Colleges in Telangana. He is author of books namely: FEA, Computer Graphics, CAD/CAM, Fuzzy Logic and Neural Networks, and Instrumentation and Controls. Number of citations are 604. His research interests include Finite Element Methods, CAD/CAM, Robotics and Characterization of Composite Materials and Manufacturing Technologies.